Blue OLEDs Utilizing Spiro[fluorene-7,9'-benzofluorene]-type Compounds as Hosts and Dopants

Joo-Han Kim, Young-Min Jeon, Ji-Geun Jang,† Sangouk Ryu,† Ho-Jung Chang,‡ Chil-Won Lee,‡ Joon-Woo Kim,‡ and Myoung-Seon Gong*

Department of Chemistry and Institute of Basic Science, Dankook University, Chungnam 330-714, Korea
**E-mail: msgong@dankook.ac.kr*
†Department of Electronic Engineering, Dankook University, Chungnam 330-714, Korea
‡OLED Team, Daejoo Electronic Materials, Siheung, Gyeonggi 429-848, Korea
Received Nobember 11, 2008, Accepted January 28, 2009

A novel spiro-type host material, 5-[4-(1-naphthyl)phenyl]-spiro[fluorene-7,9'-benzofluorene] (BH-1PN) and three new dopants, namely, 5-[diphenylamino)phenyl]-spiro[fluorene-7,9'-benzofluorene] (BH-1TPA), 5-[4-(*N*-phenyl (*m*-tolyl)amino]-spiro[fluorene-7,9'-benzofluorene] (BH-1MDPA) and 5-[(*N*-phenyl)-2-naphthyl]amino-spiro[fluorene-7,9'-benzofluorene] (BH-1NPA) were designed and successfully prepared using the Suzuki or amination reactions. The electroluminescence characteristics of BH-1PN as a blue host material doped with each of the blue dopants were evaluated. The structure of the device is ITO/DNTPD/NPB/BH-1PN:5% dopant/Alq$_3$/Al-LiF. The device obtained from BH-1PN doped with diphenyl-[4-(2-[1,1;4,1]terphenyl-4-yl-vinyl)phenyl]-amine (BD-1) showed good color purity, efficiency, luminance, and current-density characteristics.

Key Words: Blue OLED, Host, Dopant, Spiro[fluorene-7,9'-benzofluorene], Color purity

Introduction

Spiro compounds with specific steric configurations have attracted attention as organic functional materials in terms of their specific physical properties, and as a result an important class of spiro compounds with high glass transition temperatures has evolved for use as optoelectronic materials.[1-8] In particular, much of the recent research into blue light-emitting materials has centered on spiro-based derivatives, because of their high solution and solid state photoluminescence quantum yields.[3,9] A considerable amount of evidence indicates that OLEDs based on a high glass transition temperature (T_g) amorphous thin film are less vulnerable to heat damage, and hence, are more stable in use.[10-16] Thus, high T_g materials are always desirable in OLED applications. Organic conjugated materials continue to attract considerable interest because of their potential applications in optoelectronic devices. On the other hand, amorphous triarylamines, which have high glassy state stability, are suitable as hole-transporting materials in organic light emitting devices (OLED). Many attempts have been made to develop new amorphous triarylamines with high morphological stability, and the introduction of the spiro linkage has resulted in the generation of triarylamines with higher T_g values.[16,17] Asymmetric substituted triarylamines normally yield thin films of high thermal stability.[18-24] Furthermore, the primary structural feature of amorphous triarylamines that exhibits high morphological stability is a stable noncoplanar conformation, which can efficiently inhibit crystallization.[25]

To explore a complicated light-emitting system and gain better insight of the effects of spiro-substituted moieties on electronic structure, we present the designs and syntheses of a spiro-based host and of dopant materials, and the results of an investigation of their electroluminescence properties as blue light-emitting materials.

Experimental

Materials and Instruments. Tetrakis(triphenylphosphine) palladium(0), *n*-butyllithium, diphenylamine, 4-(diphenylamino) phenylboronic acid, *N*-(*m*-tolyl)phenylamine, *N*-phenyl-2-naphthylamine and potassium *t*-butoxide (Sigma-Aldrich Chem) were used as received. Palladium acetate and tri *t*-butylphosphine (TCI Chem) were used without further purification. Tetrahydrofuran and toluene were distilled over sodium and calcium hydride. 5-Bromo-spiro[fluorene-7,9'-benzofluorene] (**1**) was prepared using a previously reported method.[20]

FT-IR spectra were obtained using a Biorad Excaliber FTS-3000MX spectrophotometer, and ^{1}H NMR and ^{13}C NMR spectra were recorded on a Bruker, Avance 500 (500 MHz) spectrometer. Photoluminescence (PL) spectra were recorded on a fluorescence spectrophotometer (Jasco FP-6500) and UV-vis spectra were obtained using a UV-vis spectrophotometer (Shimadzu, UV-1601PC). Elemental analyses were performed using a CE Instrument (EA1110), and DSC measurements were performed using Mettler DSC-822e under nitrogen at a heating rate of 10 °C/min. Low and high resolution mass spectra were recorded using a mass spectrometer (JEOL, JMS-AX505WA) in FAB mode.

Synthesis of 5-[4-(1-Naphthyl)phenyl]-spiro[fluorene-7,9'-benzofluorene] (BH-1PN). Compound **1** (6.23 g, 14 mmol), 4-(naphthalene-1-yl)phenylboronic acid (3.65 g, 15 mmol) and tetrakis(triphenylphosphine)palladium(0) (0.81 g, 0.70 mmol) were dissolved in THF (100 mL) in a two-necked flask with stirring under nitrogen for 1 h. To the above reaction mixture was added a solution of potassium carbonate (2 M, 100 mL) dropwise over 30 min, and the reaction mixture was refluxed for 12 h under nitrogen. After cooling to ambient temperature, the reaction mixture was extracted with methy-

lene chloride and water. The organic layer so obtained was evaporated using a rotary evaporator, and the residue obtained subjected to column chromatography using methylene chloride/*n*-hexane (1/3) as eluent. A yellow powdery product was obtained.

Yield: 60%. Mp 339.3 °C. δ 8.86-8.82 (d, 1H, Ar-CH-benzene), 8.41-8.39 (d, 1H, Ar-CH-benzene), 8.13-8.05 (d, 1H, Ar-CH-benzene), 7.80-7.76 (t, 2H, Ar-CH-naphthalene), 7.77-7.74 (t, 2H, Ar-CH-fluorene), 7.67-7.64 (t, 2H, Ar-CH-fluorene), 7.47-7.44 (d, 1H, Ar-CH-benzene), 7.31-7.27 (t, 2H, Ar-CH-naphthalene), 7.23~7.21 (t, 2H, Ar-CH-naphthalene), 7.18~7.16 (m, 3H, Ar-CH-benzene), 7.14-7.12 (d, 1H, Ar-CH-benzene), 7.12~7.10 (t, 2H, Ar-CH-benzene), 7.10-7.08 (d, 1H, Ar-CH-benzene), 7.08-7.06 (d, 1H, Ar-CH-benzene), 7.02-7.00 (d, 1H, Ar-CH-fluorene), 7.00~6.98 (d, 1H, Ar-CH-naphthalene), 6.74~6.70 (m, 2H, Ar-CH-fluorene), 6.70-6.70 (d, 1H, CH-fluorene), 6.68~6.65 (d, 1H, Ar-CH-fluorene). FT-IR (KBr, cm^{-1}) 1600 (aromatic C=C) 3120, 880 (aromatic C-H). MS (FAB) m/z 568.0 [$(M+1)^+$]. Anal. Calcd. for $C_{45}H_{28}$ (568.22) C, 95.04; H, 4.96. Found: C, 95.01; H, 4.89. UV-vis (THF): λ_{max} (Absorption) = 351 nm, λ_{max} (Emission) = 423 nm.

Synthesis of 5-[4-(Diphenylamino)phenyl]-spiro[fluorene-7,9'-benzofluorene] (BH-1TPA). Compound **1** (6.68 g, 15 mmol), 4-(diphenylamino)phenylboronic acid (4.55 g, 16 mmol) and tetrakis(triphenylphosphine)palladium(0) (0.87 g, 0.75 mmol) were dissolved in THF (100 mL) in a two-necked flask with stirring under nitrogen for 1 h. To the above mixture, was added a solution of potassium carbonate (2 M, 100 mL) dropwise over a period of 30 min. The mixture was then refluxed for 12 h under nitrogen. After being cooled to ambient temperature, the mixture was extracted with methylene chloride and water. After evaporating the organic layer so obtained using a rotary evaporator, the residue was subjected to column chromatography using methylene chloride as eluent to give the yellow powdery product.

Yield 70 %. Mp 284.5 °C. ^{1}H NMR (500 MHz, $CDCl_3$) δ 8.86-8.82 (d, 1H), 8.42-8.40 (d, 1H), 8.14-8.02 (d, 1H), 7.80-7.76 (d, 1H), 7.77-7.74 (t, 2H), 7.67-7.64 (t, 2H), 7.47-7.44 (t, 2H), 7.41-7.37 (t, 2H), 7.17-7.09 (m, 3H), 6.89-6.88 (t, 2H), 6.87-6.84 (m, 3H), 6.82-6.81 (t, 2H), 6.80-6.78 (d, 1H), 6.77-6.75 (d, 1H), 6.74-6.70 (m, 3H), 6.70-6.70 (d, 1H), 6.69-6.67 (m, 3H) FT-IR (KBr, cm^{-1}) 3115 (aromatic C-H), 1585 (aromatic C=C), 900 (aromatic C-H), 1450, 1345 (aliphatic C-N). MS (FAB) m/z 609.0 [$(M+1)^+$]. Anal. Calcd. for $C_{47}H_{31}N$ (609.25) C, 92.58; H, 5.12; N, 2.30. Found: C, 92.51; H, 5.07; N, 2.28. UV-vis (THF): λ_{max} (Absorption) = 356 nm, λ_{max} (Emission) = 450 nm.

Synthesis of 5-[*N*-Phenyl(*m*-tolyl)amino]-spiro[fluorene-7,9'-benzofluorene] (BH-1MDPA). Compound **3** (7 g, 16 mmol), *N*-(*m*-tolyl)phenylamine (3.456 g, 19 mmol) and palladium acetate (0.106 g, 0.41 mmol) were dissolved in anhydrous toluene under nitrogen. To this mixture was slowly added a solution of tri-*t*-butylphosphine dissolved in toluene (0.5 M, 3.1 mL) and potassium *t*-butoxide (3.02 g, 31 mmol). The reaction mixture was stirred for 18 h at 100 °C, then diluted with methylene chloride, and washed with distilled water (50 mL) three times. The organic layer so obtained was dried over anhydrous $MgSO_4$ and evaporated under reduced pressure to give the crude product, which was purified by col umn chromatography using methylene chloride/*n*-hexane (2:3) as eluent.

Yield 65%. Mp 227.3 °C. ^{1}H NMR (500 MHz, $CDCl_3$) δ 8.86-8.82 (d, 1H), 8.42-8.40 (d, 1H), 8.14-8.02 (d, 1H), 7.80-7.76 (d, 1H), 7.77-7.74 (t, 2H), 7.67-7.64 (t, 2H), 7.47-7.44 (t, 2H), 7.41-7.37 (t, 2H), 7.17-7.09 (m, 3H), 6.89-6.88 (d, 1H), 6.82-6.81 (d, 1H), 6.80-6.75 (2d, 2H), 6.74-6.70 (m, 3H), 6.70-6.70 (d, 1H), 6.69-6.67 (t, 2H), 2.09 (s, 3H, Ar-CH_3). FT-IR (KBr, cm^{-1}) 3120 (aromatic C-H), 2890 (aliphatic C-H), 1600 (aromatic C=C), 900 (aromatic C-H), 1450, 1375 (aliphatic-CH_3), 1345 (aliphatic C-N). MS (FAB) m/z 547.0 [$(M+1)^+$]. Anal. Calcd. for $C_{42}H_{29}N$ (547.23) C, 92.11; H, 5.34; N, 2.56. Found: C, 92.05; H, 5.32; N, 2.48. UV-vis (THF): λ_{max} (Absorption) = 392 nm, λ_{max} (Emission) = 448 nm.

Synthesis of and 5-[(*N*-Phenyl)-2-naphthyl]amino-spiro-[fluorene-7,9'-benzofluorene] (BH-1NPA). The procedure used to synthesize BH-1NPA was similar to that used for BH-1MDPA, but with *N*-phenyl-2-naphthylamine replacing *N*-(*m*-tolyl)phenylamine.

Yield: 70%. Mp 243.4 °C. ^{1}H NMR (500 MHz, $CDCl_3$) δ 8.86-8.82 (d, 1H), 8.42-8.40 (d, 1H), 8.14-8.02 (d, 1H), 7.79-7.76 (d, 1H), 7.77-7.74 (t, 2H), 7.67-7.64 (t, 2H), 7.47-7.44 (t, 2H), 7.40-7.37 (t, 2H), 7.16-7.10 (m, 3H), 6.89-6.88 (t, 2H), 6.87-6.84 (m, 3H), 6.82-6.81 (t, 2H), 6.80-6.78 (d, 1H), 6.77-6.75 (d, 1H), 6.74-6.70 (m, 3H), 6.70-6.70 (d, 1H), 6.69-6.67 (m, 3H). FT-IR (KBr, cm^{-1}) 3120 (aromatic C-H), 1580 (aromatic C=C), 960 (aromatic C-H), 1450, 1345 (aliphatic C-N). MS (FAB) m/z 583.0 [$(M+1)^+$]. Anal. Calcd. for $C_{45}H_{29}N$ (583.23) C, 92.59; H, 5.01; N, 2.40. Found: C, 92.53; H, 4.96; N, 2.39. UV-vis (THF): λ_{max} (Absorption) = 390 nm, λ_{max} (Emission) = 468 nm.

OLED Fabrication and Measurement. Organic layers were deposited sequentially by thermal evaporation from heated alumina crucibles onto substrate an a rate of 1.0 Å/s. The thicknesses of *N,N'*-bis-[4-(di-*m*-tolylamino)phenyl]-*N,N'*-diphenylbiphenyl-4,4'-diamine (DNTPD, HIL), bis[*N*-(1-naphthyl)-*N*-phenyl]benzidine (α-NPD, HTL), host:5% dopant (EML) and Alq_3 layers were *ca.* 400, 200, 300 and 200 Å, respectively. Diphenyl-[4-(2-[1.1:4,1]terphenyl-4-yl-vinyl)phenyl]-amine (BD-1) was used as a conventional dopant. Before the deposition of a metal cathode, LiF was deposited onto the organic layers at a thickness of 10 Å. A high-purity aluminum cathode was then deposited at a rate of 1~5 Å/s to a thickness of 2000 Å as the top layer. The current-voltage characteristics of the encapsulated devices were measured using a programmable electrometer with current and voltage sources (Keithley 237 model). Luminance and EL spectra were measured using a PR650 system (Photo Research Co. Ltd.).

Results and Discussion

Synthesis and Characterization. The Suzuki and amination reactions were used to obtain the various spiro-type hosts and dopants, namely, BH-1PN, BH-1TPA, BH-1MDPA and BH-1TPA, as shown in Scheme 1. BH-1PN host material and

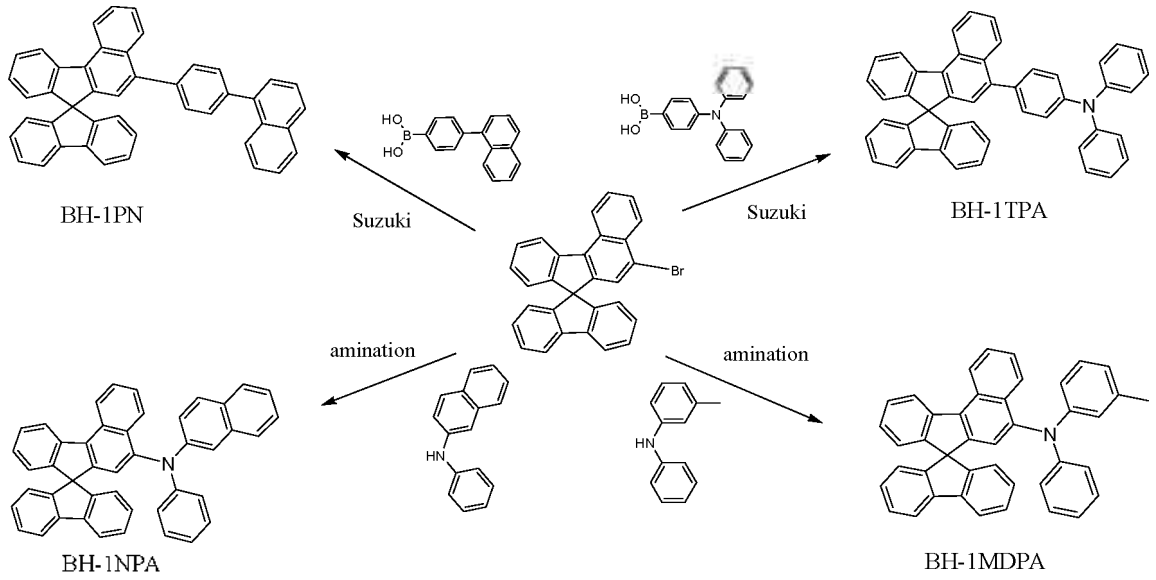

Scheme 1. Synthetic scheme of host and dopants.

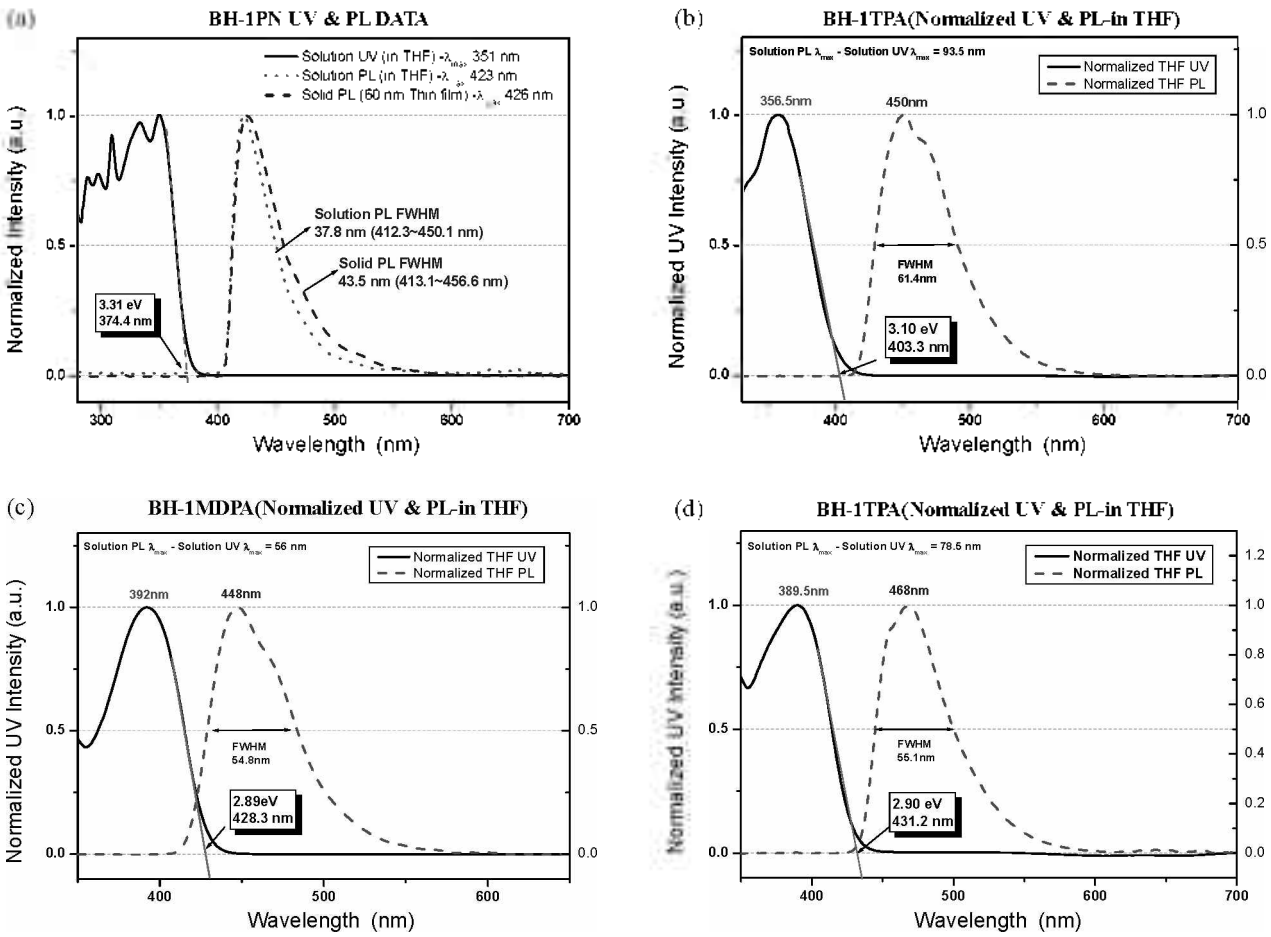

Figure 1. Normalized absorption and photoluminescence spectra of (a) BH-1PN, (b) BH-1TPA, (c) BH-1MDPA and (d) BH-1NPA.

BH-1TPA dopant were prepared by the Suzuki reaction between **1** and 4-(naphthalen-1-yl)phenylboronic acid or 4-(diphenylamiono)phenylboronic acid in the presence of a palladium catalyst, respectively. Blue dopants, BH-1MDPA and BH-1NPA were synthesized by reacting **1** with *N*-phenyl (*m*-tolyl)amine or *N*-phenyl-2-naphthylamine in the presence of palladium catalyst, respectively. The chemical structures and compositions of the resulting precursor and the spiro-compounds were characterized by ^{1}H NMR, ^{13}C NMR, FT-IR, GC-MS and by elemental analysis.

Table 1. Thermal properties of new host and dopant materials

	Temp (°C)	BH-1PN	BH-1MDPA	BH-1TPA	BH-1NPA	BD-1
Thermal properties	T_g[a]	171.0	-	-	-	-
	T_m[b]	339.3	227.3	284.5	243.4	306.9

[a]Glass transition temperature: [b]Melting temperature

Table 2. Optical properties new host and dopant materials

Properties \ Host, dopant		BH-1PN	BD-1	BH-1TPA	BH-1MDPA	BH-1NPA
Abs (THF)	nm	350	383	356.5	392	389.5
Em (THF)	nm	423	451	450	448	468
Em (Film)	nm	426	-	445	452	465
FWHM	nm	43	68.5	60	59	59
HOMO	eV	5.95	5.44	5.58	5.62	5.56
LUMO	eV	2.64	2.57	2.48	2.72	2.66
Band gap	eV	3.31	2.96	3.10	2.90	2.90

Optical Properties. UV-vis and photoluminescence (PL) spectra of the spiro compounds are shown in Figure 1. In the case of BH-1PN host material, maximum absorption in the UV-vis spectrum was observed at λ_{max}= 351 nm in THF and the PL emission peak was at 423 nm. BH-1TPA showed a UV-vis absorption maximum at 356 nm and with an onset at 374.3 nm (corresponding to a band gap energy of 3.31 eV), whereas BH-1NPA showed a UV absorption maximum at 390 nm and an onset at 431.2 nm. BH-1MDPA dopant had a λ_{max} at 392 nm due to a $\pi \rightarrow \pi^*$ transition derived from the conjugated substituted diphenylamine group. The PL maximum absorptions of BH-1TPA, BH-1NPA and BH-1MDPA were located at 448, 468 and 450 nm in the typical blue region.

Thermal Properties. Differential scanning calorimetry (DSC) was performed to investigate the thermal properties of BH-1PN, BH-1NPA, BH-1TPA, and BH-1MDPA, findings are summarized in Table 1. The purified sample of BH-1PN revealed a melting point (T_m) at 339.3 °C after sublimation. After the sample had cooled to room temperature, a second DSC at 10 °C/min revealed a high glass transition temperature (T_g) of 171.0 °C. This result implied that the introduction of naphthylphenyl moiety improved thermal stability significantly. DSC data of BH-1TPA, BH-1MDPA and BH-1NPA revealed melting temperatures (T_m) of 284.5, 243.3, and 227.3 °C, respectively. BH-1TPA is more thermally stable than BH-1MDPA and BH-1NPA because it has a more symmetric structure and a higher molecular weight due to the presence of an additional phenylene group.

Energy Levels of HOMO and LUMO of Materials. A low-energy photo-electron spectrometer was used to obtain information about the HOMO and LUMO energy values of host and dopants and to examine charge injection barriers. The optical energy band gap of BH-1PN was estimated to be 3.31 eV based on the energy threshold of its electronic absorption spectrum (Figure 1(a)). The LUMO energy level of BH-1PN was estimated to be 2.64 eV, and its HOMO energy level to be 5.95 eV, as estimated from its optical band gap. The energy levels of BH-1TPA, BH-1MDPA, and BH-1NPA are shown in Table 2.

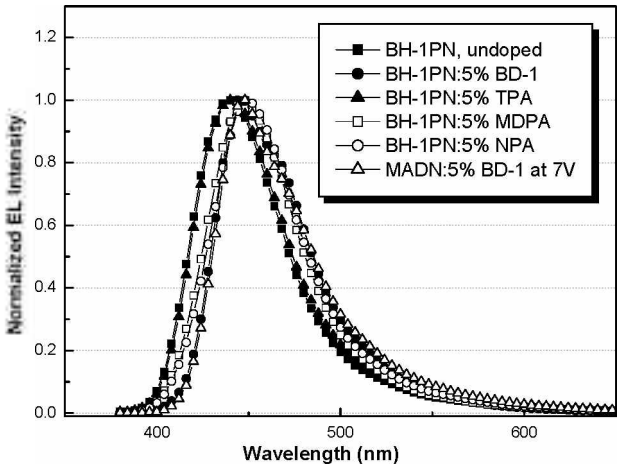

Figure 2. EL spectra of the devices composed of BH-1PN:5% dopants.

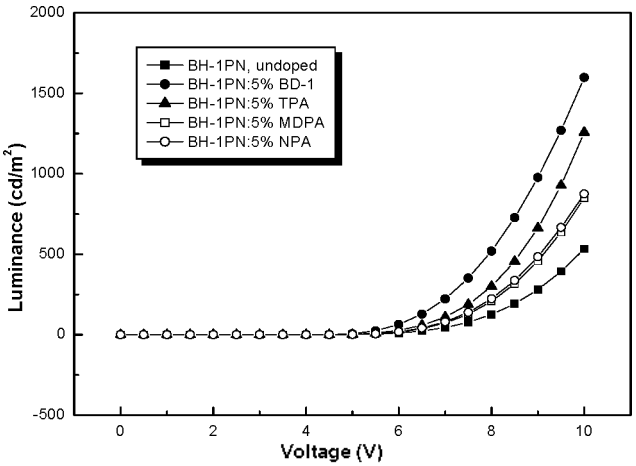

Figure 3. Brightness-voltage characteristics of the device composed of BH-1PN:5% dopants.

EL Properties. To study the EL properties of BH-1PN, multilayer devices with the configuration of glass ITO anode/hole injection layer (HIL)/hole transport layer (HTL)/emitting layer (EML)/electron transport layer (ETL)/electron injection layer (EIL)/Al cathode were fabricated. DNTPD was used as the HIL, α-NPD as the HTL, BH-1PN:5% dopant as the EML and Alq3 as the ETL; 10 Å LiF was used as the EIL.

Figure 2 shows the EL spectra of a device composed of BH-1PN doped with various dopants at 7 V. Most of the EL spectral activity occurred at 440-445 nm. The EL spectra correlated well with the PL spectra of BH-1PN. Based on the EL spectrum, CIE coordinates of the emitting layer BH-1PN doped with 5% TPA were measured to be 0.15 and 0.09. The device composed of BH-1PN without dopant showed an EL spectrum at 440nm while the other EL spectra were shifted by 5 nm toward longer wavelengths. The emitting color of the device comprised of BH-1PN:5% BD-1, BH-1MDPA, BH-1NPA and BH-1PN without dopant in the emitting layer

Table 3. EL properties of the devices obtained from BH-1PN host with various dopant materials

Properties \ Devices[a]		1	2	3	4	5
EL at 7V	mA/cm^2	0.01	0.02	8.79	4.61	5.16
	cd/A	1.00	2.81	1.24	1.58	1.55
	cd/m^2	44.26	222.4	109.3	72.66	80.15
	CIE-x	0.16	0.15	0.16	0.15	0.15
	CIE-y	0.08	0.10	0.09	0.09	0.10

[a]1, BH-1PN; 2, BH-1PN:5%BD-1; 3, BH-1PN:5%BH-1TPA; 4, BH-1PN:5%BH-1MDPA; 5, BH-1PN:5%BH-1NPA

showed deep blue emission (x,y) = (0.15, 0.10), (0.16, 0.09), (0.15, 0.09), (0.15, 0.10) and (0.16, 0.08), respectively, in terms of CIE chromaticity coordinates. A comparison of the CIE coordinates of the emissions of optimal devices containing MADN:5% BD-1 revealed that devices containing BH-1PN had better color saturations, i.e., BH-1PN CIE coordinates were better than those of MADN (0.15, 0.12).

OLED Device Properties. Performance differences between devices comprised of BH-1PN or various 5% dopants are clearly demonstrated by the luminance behaviors shown in Figure 3. The initial light outputs of the devices occurred at around 6.0 V. Maximum luminance values of 1598, 1257, 849, 874 and 533 cd/m^2 at 10 V were observed for Device 1 (undoped), Device 2 (BD-1), Device 3 (BH-1DPA) and Device 4 (BH-1MDP, and for Device 5 (BH-1NPA), respectively. The details of the EL performances of these devices are listed in Table 3. The ITO/DNTPD/NPB/BH-1PN:5% BH-TPA/Alq_3/Al-LiF device showed an EL absorption maximum at 447.8 nm, and its luminance increased from 533 cd/m^2 (Device 5) to 1598 cd/m^2.

The current efficiency-voltage characteristics of the five devices are presented in Figure 4. Charge injection starting to emit light from these devices was at around 4.2 V. Device 1 using BH-1PN:5% BD-1 had the greatest current efficiency of 2.91 cd/A. It was obvious that the luminance efficiencies of devices made using BD-1 were greater than those of devices made using the other dopants. Evidently, BH-1PN itself has low luminance and luminance efficiency, which is probably due to a thin emission layer that leads to leakage of un-recombined carriers or luminescence quenching. Thus, Alq_3 was required as an electron transporting material to shift the recombination zone from the electrodes and to reduce radiative quenching.

The current density-voltage characteristics of the OLEDs doped with various dopants are presented in Figure 5. The voltage-current density characteristics of the devices with the structure, ITO/DNTPD/α-NPD/BH-1PN:5% dopant/Alq_3/Al-LiF, exhibited typical diode behavior and their luminances were strongly influenced by dopants, as shown in Figure 5. It was found that devices derived from BH-1PN showed low current densities. At a driving voltage of 7 and 10 V, current densities reached 8.8 and 106.5 mA/cm^2 for Device 3 using BH-1PN:5% BH-1TPA, respectively. Unsatisfactorily, somewhat higher turn-on voltages were measured for BH-1PN: BD-1 than MADN:BD-1 at same doping levels. These higher

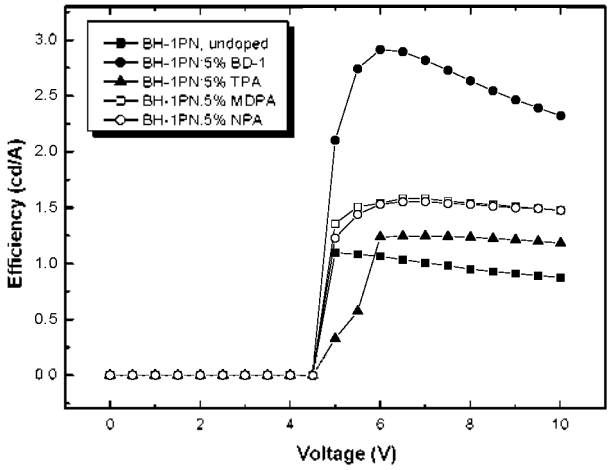

Figure 4. Efficiency-voltage characteristics of the device using BH-1PN:5% dopants.

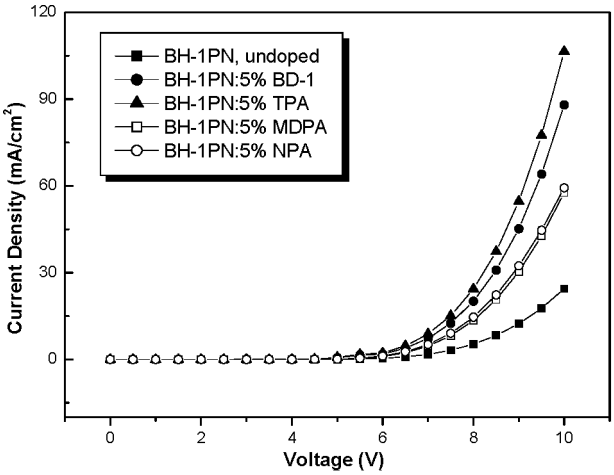

Figure 5. Current density-voltage characteristics of BH-1PN 1PN: 5% dopants.

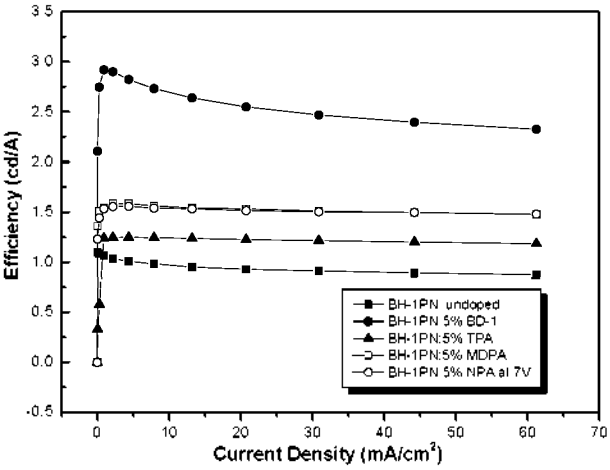

Figure 6. Efficiency-current density characteristics of the device using BH-1PN:5% dopants.

turn-on voltages were presumably due to the increasing electron injection barrier of BH-1PN, which concurs with its higher LUMO level.

Figure 6 shows current density-dependent variations of luminance efficiencies for a series of BH-1PN host devices doped with 5% BD-1, BH-1TPA, BH-1MDPA, or BH-1NPA and for undoped BH-1PN. Details of the EL performances of these devices are shown in Table 3. The devices were found to be less susceptible to current-induced quenching up to a current density of 60 mA/cm^2, and consequently, devices comprised of BH-1PN:5% BD-1 maintained a efficiency of 2.50 cd/A throughout the measured current density range. As current density was increased gradually, emitting efficiency increased rapidly. This implies that an exciton is formed and light is emitted at specific thresholds. It should be noted that the efficiencies of these devices remain stable when the current density is increased from 5 to 60 mA/cm^2 (Figure 6).

Conclusion

A new blue spiro-type host material BH-1PN and three new blue spiro-type dopants BH-1NPA, BH-1TPA and BH-1MDPA were prepared and used as host and dopants to construct blue OLEDs. OLEDs composed of BH-1PN as a host with the structure, ITO/DNTPD/α-NPD/BH-1PN:5% dopant/Alq_3/Al-LiF, were fabricated and characterized. In optimized structures, the device obtained using BH-1PN:5% BD-1 had greatest luminance at 1598 cd/m^2, at a current density of 106.5 mA/cm^2 being 2.91 cd/A with color coordinates of 0.15 and 0.09.

Acknowledgments. This work was supported by the Regional Technology Innovation program of the Korean Ministry of Knowledge Economy (MKE) (#RT104-01-02).

Reference

1. Saragi, T. P. I.; Spehr, T.; Siebert, A.; Fuhrmann, L. T.; Salbeck, J. *Chem. Rev.* **2007**, *107*, 1011.
2. Xiao, H.; Shen, H.; Lin, Y.; Su, J. *Dyes and Pigments* **2007**, *73*, 224.
3. Chen, C. T.; Wei, Y.; Lin, J. S.; Moturu, M. V. R. K.; Chao, W. S.; Tao, Y. T.; Chien, C. H. *J. Am. Chem. Soc.* **2006**, *128*, 10992.
4. Pei, J.; Ni, J.; Zhou, X. H.; Cao, X. Y.; Lai, Y. H. *J. Org. Chem.* **2002**, *67*, 4924.
5. Fournier, J. H.; Maris, T.; Wuest, J. D. *J. Org. Chem.* **2004**, *69*, 1762.
6. Wong, K. T.; Wang, Z. J.; Chien, Y. Y.; Wang, C. L. *Org. Lett.* **2001**, *3*, 2285.
7. Horhant, D.; Liang, J. J.; Virboul, M.; Poriel, C.; Alcaraz, G.; Rault-Berthelot, J. *Org. Lett.* **2006**, *8*, 257.
8. Lee, H.; Oh, J.; Chu, H. Y.; Lee, J. I.; Kim, S. H.; Yang, Y. S.; Kim, G. H.; Do, I. M.; Zyung, T.; Lee, J.; Park, Y. *Tetrahedron* **2003**, *59*, 2773.
9. Wang, K. T.; Wang, C. L. *Org. Lett.* **2001**, *3*, 2285.
10. Naito, K.; Miura, A. *J. Phys. Chem.* **1993**, *97*, 6240.
11. Tokito, S.; Tanaka, H.; Noda, K.; Okada, A.; Taga, Y. *Appl. Phys. Lett.* **1997**, *70*, 1929.
12. Salbeck, J.; Yu, N.; Bauer, J.; Weissörtel, F.; Bestgen, H. *Synth. Met.* **1997**, *91*, 209.
13. Konne, B. E.; Loy, D. E.; Thompson, M. E. *Chem. Mater.* **1998**, *10*, 2235.
14. O'Brien, D. F.; Burrows, P. E.; Forrest, S. R.; Konne, B. E.; Loy, D. E.; Thompson, M. E. *Adv. Mater.* **1998**, *10*, 1108.
15. Steuber, F.; Staudigel, J.; Stössel, M.; Simmerer, J.; Winnacker, A.; Spreitzer, H.; Weissörtel, F.; Salbeck, J. *Adv. Mater.* **2000**, *12*, 130.
16. Shirota, Y. *J. Mater. Chem.* **2000**, *10*, 1.
17. Strohriegl, P.; Grazulevicius, J. V. *Adv. Mater.* **2002**, *14*, 1439.
18. Koene, B. E.; Loy, D. E.; Thompson, M. E. *Chem. Mater.* **1998**, *10*, 2235.
19. Nizhegorodov, N. I.; Downey, W. S. *J. Phys. Chem.* **1994**, *98*, 5639.
20. Jeon, S. O.; Jeon, Y. M.; Kim, J. W.; Lee, C. W.; Gong, M. S. *Org. Electron.* **2008**, *9*, 522.
21. Kim, K. S.; Jeon, Y. M.; Kim, J. W.; Lee, C. W.; Gong, M. S. *Org. Electron.* **2008**, *9*, 797.
22. Kim, K. S.; Jeon, Y. M.; Kim, J. W.; Lee, C. W.; Gong, M. S. *Synth. Met.* **2008**, *158*, 870.
23. Kim, K. S.; Jeon, Y. M.; Kim, J. W.; Lee, C. W.; Gong, M. S. *Dyes and Pigments* **2009**, *81*, 174.
24. Jeon, S. O.; Lee, H. S.; Jeon, Y. M.; Kim, J. W.; Lee, C. W.; Gong, M. S. *Bull. Korean Chem. Soc.* **2009**, in press.
25. Wong, K. T.; Wang, Z. J.; Chien, Y. Y.; Wang, C. L. *Org. Lett.* **2001**, *3*, 2285.